

# Adsorption geometry of hydrogen on Fe (110)

W. Moritz<sup>a)</sup>

*Institut für Kristallographie, Universität München, 8 München 2, West Germany*

R. Imbihl,<sup>b)</sup> R. J. Behm, G. Ertl, and T. Matsushima<sup>c)</sup>

*Institut für Physikalische Chemie, Universität München, 8 München 2, West Germany*

(Received 21 February 1985; accepted 3 May 1985)

From an analysis of the low-energy electron diffraction (LEED) intensities we have determined the adsorption geometry of the two ordered H adlayers formed at  $T < 270$  K on Fe (110): a  $(2 \times 1)$  and a  $(3 \times 1)$  structure, with ideal coverages of  $\theta = \frac{1}{2}$  and  $\theta = \frac{2}{3}$ . Calculations were performed for different adsorption sites and structural models, taking the Fe–H bond length and the first Fe–Fe interlayer spacing as variable parameters. An  $R$  factor analysis was used for quantitative comparison with the experimental data. In both structures the H atoms are adsorbed on highly coordinated (i.e., quasithreefold) sites: The  $R$  factors of *only* the superlattice beams ( $R_{\text{Zanazzi-Jona}} = 0.26$ ,  $R_{\text{Pendry}} = 0.55$  in the  $(2 \times 1)$  and  $R_{\text{ZJ}} = 0.4$ ,  $R_{\text{P}} = 0.58$  in the  $(3 \times 1)$  structure) are significantly lower than those from models with a long bridge adsorption site ( $R_{\text{ZJ}} = 0.37$ ,  $R_{\text{P}} = 0.66$  and  $R_{\text{ZJ}} = 0.6$ ,  $R_{\text{P}} = 0.74$ ). The on top site and the short bridge site can clearly be ruled out. For both structures the minima occur at the same Fe–H interlayer spacing of  $0.9 \pm 0.1$  Å, equivalent to an Fe–H distance of  $1.75 \pm 0.05$  Å or  $r_{\text{H}} = 0.47 \pm 0.05$  Å. From the  $R$  factor minimum of all beams ( $R_{\text{ZJ}} = 0.23$ ,  $R_{\text{P}} = 0.46$ ) the first Fe–Fe interlayer spacing is found to be equal to its bulk value, like on the clean surface. In the  $(2 \times 1)$  structure the only possible arrangement of the  $\text{H}_{\text{ad}}$  atoms consists of dense packed rows in [001] direction which are separated by a row of unoccupied sites, respectively, due to a delocalization of the H atoms over two neighboring threefold sites, short-range fluctuations can be envisaged. Their influence upon  $I/V$  curves and relative intensities of different superlattice beams was analyzed. As a result this effect could be excluded, large domains are required, in which only one type of threefold sites is occupied. For the  $(3 \times 1)$  structure a model is favored in which the lateral distribution of the adatoms differs from a previous suggestion. It is shown that this model is more plausible in view of the H–H interactions. The higher density of threefold sites also has implications for the discussion of the 2D phase diagram of H/Fe (110), especially on the requirement of trio interactions.

## I. INTRODUCTION

The interaction of hydrogen with transition-metal surfaces has already been the subject of numerous investigations<sup>1</sup> which also include studies with clean iron surfaces.<sup>2–6</sup> In all cases  $\text{H}_2$  adsorbs dissociatively with a chemisorption energy of around 20 kcal/mol. On Fe (110) the adsorbed H atoms form below  $\sim 250$  K two ordered structures, a  $(2 \times 1)$  and a  $(3 \times 1)$  structure (depending on coverage), as determined by low-energy electron diffraction (LEED).<sup>2</sup> The present work was concerned with the analysis of these structures on the basis of a quantitative evaluation of LEED intensity/voltage ( $I/V$ ) data.

Previous investigations of this system were concerned with the experimental determination of the phase diagram of the two ordered structures and of the stability region of anti-phase domains on the basis of LEED intensity and beam profile measurements.<sup>6</sup> The  $(2 \times 1)$  structure has its maximum intensity (i.e., optimum order) at a H coverage of

$\theta = 0.5$ , the  $(3 \times 1)$  structure at  $\theta = 0.66$ . This phase diagram subsequently was subject of extensive theoretical work<sup>7–10</sup> in which it could be satisfactorily modeled by properly adjusting the interaction energies between adsorbed particles. Direct access to these interaction energies was obtained in the embedded-cluster calculations by Muscat<sup>11</sup> from whose work also the threefold adsorption site was concluded to be energetically most favorable. This conclusion is in contrast to the previously proposed long bridge site<sup>2,6</sup> which was also assumed in the statistical treatments of the phase diagram,<sup>7–10</sup> but would be in agreement with the general experience with other systems [e.g., H/Ni (111),<sup>12</sup> H/Ni (110),<sup>13–15</sup> H/Pt (111)<sup>16,17</sup>] where evidence exists that the adsorbed H atoms prefer the sites with highest coordination.

The results of the LEED analysis presented in this paper will demonstrate that also with H/Fe (110) there is indeed strong evidence for the occupation of the highly coordinated (i.e., threefold) adsorption sites. In addition, for the  $(3 \times 1)$  structure a model will be favored in which the lateral distribution of the adparticles differs from the previous suggestions.

## II. EXPERIMENTAL

The experiments were performed in a standard UHV system (base pressure below  $10^{-10}$  Torr) equipped with faci-

<sup>a)</sup> Present address: University of Wisconsin, Department of Materials Science, Madison, Wisconsin 53706.

<sup>b)</sup> Present address: IBM Thomas J. Watson Research Center, Yorktown Heights, New York 10598.

<sup>c)</sup> Present address: Hokkaido University, Research Institute for Catalysis, Sapporo, Japan.

lities for LEED, Auger Electron Spectroscopy (AES), and Thermal Desorption measurements. The sample was cut from a single crystal rod (purity 99.99%, Metals Research) after being oriented by x-ray diffraction. It was mechanically polished to give a mirror finish for the surface and finally the orientation was checked to be within  $\pm 0.5^\circ$  of the [110] direction. The cleaning, which proved to be very tedious, consisted of oxidation-sputtering cycles, after the sample had been depleted from *S* and *P* by sputtering at elevated temperatures. Details of the cleaning procedure have been published earlier.<sup>2</sup> In order to achieve well-developed hydrogen superstructures, the impurity level of the main contaminants, carbon and oxygen, had to be kept well below 5% of a monolayer. This was checked by AES and, more reliably with respect to the quality of the ordered structures, by measuring the intensities and beam profiles of the respective hydrogen superstructure beams. The overlayer structures were prepared by subsequently exposing the sample at 110 K to  $H_2$  and annealing to 280 K, until the maximum intensity of the extra beams was reached. The annealing procedure was necessary to dissolve metastable structures that can build up upon adsorption at low temperatures. The width of the extra beams was comparable to that of the integral order beams indicating domains with a size exceeding 100 Å.  $I/V$  spectra were recorded at 110 K with a moveable Faraday cup (aperture 1.4°) and by means of a computer controlled video system directly measuring the spot intensity on the LEED screen.<sup>18</sup> A comparison between  $I/V$  curves measured by both techniques showed only deviations in the low-energy range of the respective beams. In this case the spots are near the edge of the LEED screen and the intensities measured by the video system, which only sees the projection of the spots, is too low in this regime by up to a factor of 2 to 3. These deviations have not been corrected since, because of the very smooth change with energy, the *R* factor analysis did not react sensitively on this effect. A system of Helmholtz coils was used to compensate magnetic fields, a magnetic field probe controlled the current in the coils and reduced field variations to  $\pm 1$  mG. The field between the sample and the LEED system was regulated such that at normal incidence symmetrically equivalent beams exhibited identical  $I/V$  curves over wide energy ranges. This method was also used to adjust the angle of incidence.

### III. CALCULATIONS

The (110) face of a bcc lattice exhibits four possible adsorption sites maintaining at least one-symmetry element. These are the "top site" and "long bridge site" having 2 mm symmetry, the "short bridge site" on a twofold axis and a "quasithreefold site" on a mirror plane, as illustrated in Fig. 1. For the latter site the three surrounding Fe atoms do not form an equilateral triangle, nevertheless, we will in the following denote this a threefold hollow site.

Before starting the intensity analysis for the adsorbate system the clean surface was investigated. The results are very close to those already reported by Shih *et al.*<sup>19</sup> and are therefore not repeated here. A minimum Zanazzi–Jona *R* factor of  $R_{ZJ} = 0.16$  (see below) was achieved, no contrac-

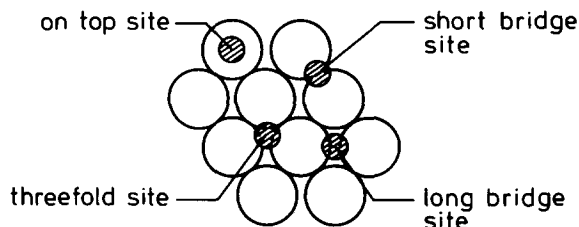


FIG. 1. H adsorption sites on Fe(110), nomenclature as indicated in the figure (open circles: Fe atoms in topmost layer, filled circles: H atoms).

tion of the top layer spacing could be found within the error limits. The inner potential was assumed to be independent of energy and the optimum value found was  $V_0 = -11$  eV. The LEED intensity analysis for the overlayer was carried out in two steps. First, calculations at normal incidence were performed to rule out certain possible adsorption sites. These were the top site and the short bridge site, as shown below. Further calculations at oblique incidence were only performed for the remaining two models. Thermal desorption studies<sup>2</sup> and EELS measurements<sup>5</sup> led to the conclusion that in both structures,  $(2 \times 1)$  and  $(3 \times 1)$ , the same adsorption site is occupied. Therefore, calculations for the short bridge site were not repeated with the  $(3 \times 1)$  structure. However, the top site model, for which calculations are easily done, was considered here too, in order to obtain more confidence about the adsorption geometry.

Due to the low scattering power of hydrogen, the fractional order beams are weak and the integral order beams are only slightly changed upon adsorption. This is also reflected in the calculated spectra, viz. the integral order beams remain nearly unchanged, independent of adsorption site or geometry of hydrogen. All beams—integral as well as fractional order beams—exhibit a strong dependence of the first bulk interlayer spacing. The substrate lattice geometry has therefore been fixed by the minimum of the *R* factor of all beams. In contrast the fractional order beams were used to determine the adsorption geometry. The weak influence of hydrogen adsorption on the  $I/V$  spectra of integer order beams is illustrated in Fig. 2.

The LEED intensity calculations themselves were performed using the layer doubling and the RFS scheme for interlayer multiple scattering.<sup>20</sup> In those models where the hydrogen atom was too close to the topmost iron layer (less than 0.8 Å) the multiple-scattering equations were solved in angular momentum space for a combined layer. The number of angular momentum components as well as the number of atoms in the unit cell was reduced by the use of symmetry adapted functions since the summation over symmetrically equivalent positions in a unit cell can be performed prior to inversion of the matrix.<sup>21</sup>

Phase shifts for iron were obtained from a self-consistent Hartree–Fock–Slater potential,<sup>22</sup> the validity of which has been already shown in previous LEED intensity calculations for the clean (100), (110), (111) faces of iron.<sup>23,19,24</sup>

A reliable procedure to construct a muffin–tin potential for H is not available. In this case the muffin–tin approximation is obviously not appropriate since the electron density of the adsorbed hydrogen atom is certainly far away from the

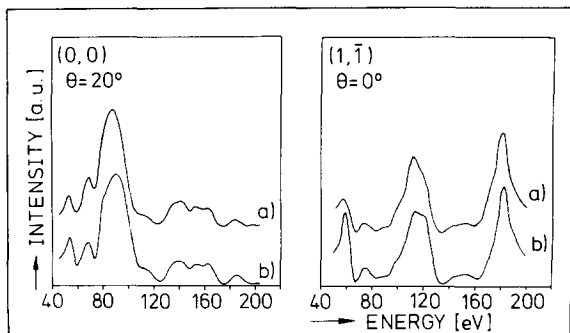


FIG. 2. Intensity of the (0,0) beam and the  $(1, \bar{1})$  beam for clean Fe (110) and the Fe surface covered by a  $(2 \times 1)$  hydrogen adlayer ( $T = 110$  K,  $\varphi = 90^\circ$ ,  $\theta = 0^\circ$  for the  $(1, \bar{1})$  beam and  $\theta = 20^\circ$  for the (0,0) beam).

free-atom electron density and not spherically symmetric. So far only one LEED intensity analysis for hydrogen adsorption has been published, namely for H/Ni (111).<sup>12</sup> There a truncated free-atom potential was used and three sets of phase shifts have been tested which had been obtained by cutting off the potential at different radii (0.7, 1.0, 1.5 a.u.). Additionally, different approximations to account for the exchange term were used and the Slater exchange approximation proved to be sufficient. The optimum radius was found at about 1 a.u. (0.529 Å), the corresponding set of phase shifts gave the most confident results. The identical procedure was applied in the present work and also led to the same result. However, not all calculations were performed with three sets of phase shifts. This was only done for the  $(2 \times 1)$  structure at normal incidence. All further calculations were performed using a muffin tin radius of 1.0 a.u., which also compares well to the bond lengths found here and for H/Ni (111).

The muffin-tin zero was kept independent of energy and was set to  $-11$  eV within the hydrogen and iron layers. The value for the inner potential was found for the clean Fe (110) surface and does not include corrections due to the work function difference between the surface and the LEED gun filament. The imaginary part of the inner potential was taken energy dependent by  $V_i = 0.85 * (E + V_0)^{1/3}$ , a value which has been found to give satisfactory results for Fe (100)<sup>25</sup> and the thermal vibrations were represented by a Debye temperature of 467 K<sup>26</sup> for all layers.

Two  $R$  factors were used for quantitative comparison of experimental and theoretical spectra. The two  $R$  factors  $R_{ZJ}$  and  $R_p$  were used as defined by the authors—Zanazzi and Jona<sup>27</sup> and Pendry.<sup>28</sup>  $R_p$  is by a factor of about 2 larger than  $R_{ZJ}$  for the same level of confidence.

#### IV. RESULTS

First, a note has to be made with respect to the nomenclature of the superstructures. We refer here to unit-cell vectors  $[001]$  and  $[\bar{1}\bar{1}\bar{1}]$  (see Fig. 3) to obtain an easy description of the superstructure cells. By reference to the primitive unit-cell vectors  $[\bar{1}11]$  and  $[1\bar{1}\bar{1}]$  the  $(2 \times 1)$  structure would be a  $c(2 \times 2)$  structure, a designation which is also widely used. The  $(2 \times 1)$  structure of hydrogen on Fe (110) should not be mixed up with the  $(2 \times 1)$  structure on W (110), where reference is made to the usual primitive unit-cell vectors.<sup>29</sup>

The  $(3 \times 1)$  structure has been called  $(3 \times 3) 6H$  in a previous paper.<sup>6</sup>

#### A. $(2 \times 1)$ structure

A total of 18 experimental spectra were compared with calculated data, nine integer and nine half-order beams. In all calculations the first bulk interlayer spacing was varied from 1.9 to 2.2 Å in steps of 0.05 Å. The H-Fe bond length was varied within a wide range from 1.5–2.2 Å. This corresponds for the on top position to an interlayer spacing of  $d_{\text{Fe-H}} = 1.5\text{--}2.2$  Å, for the short bridge site to  $d_{\text{Fe-H}} = 1.0\text{--}1.7$  Å, for the long bridge site and for the threefold hollow site approximately to  $d_{\text{Fe-H}} = 0.1\text{--}1.0$  Å. The H-Fe interlayer spacing was varied in steps of 0.2 Å and for some regions in steps of 0.1 Å.

Structure models for the long bridge site and the threefold site are shown in Fig. 3(a) and 3(b). The latter requires two domains to obtain the full 2 mm symmetry of the diffraction pattern; the dashed line in Fig. 3(b) indicates a domain boundary.

The comparison between experimental and theoretical spectra at normal incidence for the four different adsorption sites—each with its optimum parameters—is shown in Fig. 4. Integer order beams, as the (0,1) beam shown here, are nearly unaffected by the change of the position of the hydro-

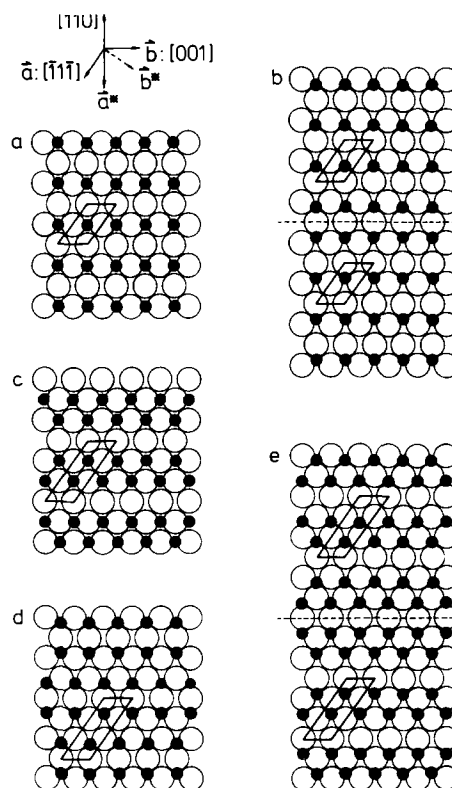


FIG. 3. Models for the  $(2 \times 1)$  and  $(3 \times 1)$  structures of adsorbed hydrogen on Fe (110); (a)  $(2 \times 1)$  structure on long bridge sites; (b)  $(2 \times 1)$  structure on threefold sites, two domains are separated by a mirror plane (dashed lines); (c)  $(3 \times 1)$  structure on long bridge sites, one domain; (d)  $(3 \times 1)$  structure on threefold sites, one domain (model I); (e)  $(3 \times 1)$  structure on threefold sites, two domains are separated by a mirror plane (dashed line) (model II).

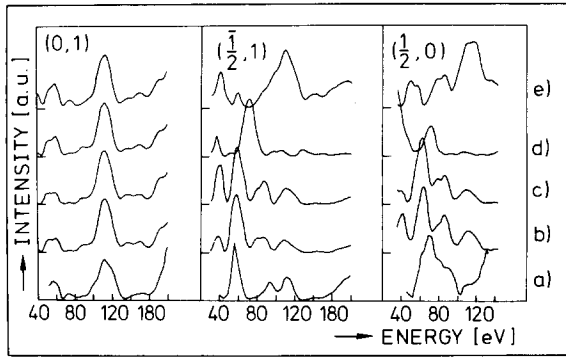


FIG. 4.  $I/V$  curves at normal incidence for the  $(2 \times 1)$  structure. (a) experimental, (b)–(e) calculated for different adsorption sites at their respective best fit Fe–H layer spacing,  $d_{\text{Fe}} - d_{\text{Fe}} = 2.0 \text{ \AA}$ ; (b) threefold site,  $d_{\text{Fe-H}} = 1.0 \text{ \AA}$ ; (c) long bridge site,  $d_{\text{Fe-H}} = 1.0 \text{ \AA}$ ; (d) short bridge site,  $d_{\text{Fe-H}} = 1.2 \text{ \AA}$ ; (e) on top site,  $d_{\text{Fe-H}} = 1.7 \text{ \AA}$ .

gen atom, therefore only superstructure beams can be used to determine the adsorption geometry of hydrogen. Clearly the on top and short bridge sites can be ruled out by visual comparison of experimental and calculated data in Fig. 4.

A decision between the remaining two sites, the long bridge site and the threefold hollow site, is much more difficult. The differences between the calculated curves for the two possible models are smaller than the differences to the experiment. Further calculations at oblique incidence were therefore performed for both models. At oblique incidence within the mirror plane the threefold site models require two calculations, one for each domain.

The similarities between theoretical spectra for both models persist at all other angles of incidence investigated here. These were the  $(\frac{1}{2}, 0)$  and the  $(\frac{1}{2}, 1)$  beams at  $\theta = 6.1^\circ$  and  $15^\circ$  and the  $(\frac{1}{2}, 0)$  and the  $(\frac{1}{2}, 1)$  beams at  $\theta = 20^\circ$  and  $25.8^\circ$ , respectively. The azimuthal angle was kept constant at  $\varphi = 90^\circ$ . Comparison of both model calculations with the experiment for most of the superstructure beams and some integer order beams at oblique incidence is shown in Fig. 5. The agreement between experimental and theoretical spectra is generally better at lower energies than at higher energies. This may be caused by two effects: One is that the experimental error increases at higher energies since the intensities are very low so that very small peaks may be due to noise in the video signal. Secondly the hydrogen atoms may occupy not only a single adsorption site but are either statically or dynamically distributed over the two possible threefold sites in the unit cell. This would lead to an anisotropic temperature factor, the influence of which increases with increasing energy. We will discuss this question in more detail later.

Visual comparison of all curves leads to approximately the same degree of confidence for both models. However, the  $R$  factor curves clearly show a preference for the threefold site. The averaged  $R$  factor curves as a function of  $d_{\text{Fe-Fe}}$  (all beams used) and  $d_{\text{Fe-H}}$  (only superlattice beams used) are shown in Figs. 6 and 7. For the threefold site both  $R$  factors exhibit minima at about the same interlayer spacing  $d_{\text{Fe-H}} = 0.8\text{--}1.0 \text{ \AA}$ , the minimum values are  $R_{\text{ZJ}} = 0.26$  and  $R_{\text{P}} = 0.55$ . For the long bridge site both  $R$  factors have minima

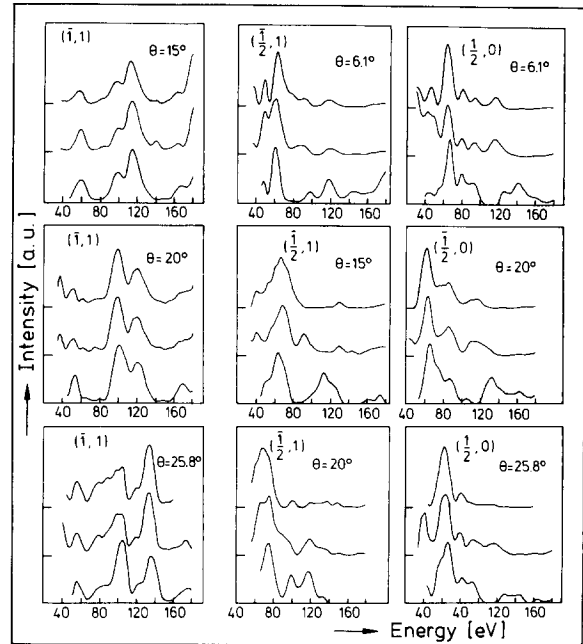


FIG. 5.  $I/V$  curves of the  $(2 \times 1)$  structure for nonnormal incidence, beams and incident polar angles as indicated,  $\varphi = 90^\circ$  (lower curve: experimental, middle curve: threefold site as in 3(b) upper curve: long bridge site as in 3(a). Fe–Fe and Fe–H optimized at  $d_{\text{Fe-Fe}} = 2.0 \text{ \AA}$  and  $d_{\text{Fe-H}} = 1.0 \text{ \AA}$ .

at different interlayer spacings and the absolute values are always larger than for the threefold site. The difference in the  $R$  factors is large enough to be significant. On the other hand, it should be noted that both models produce very similar theoretical curves and that by visual comparison alone a clear preference for one model would not be found. The similarity between both theoretical models is easily understandable by the fact that differences are only the result of multiple

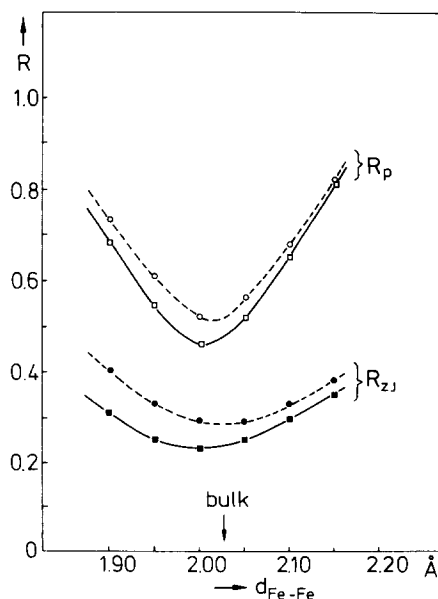


FIG. 6. Averaged  $R$  factor ( $R_{\text{ZJ}}$ : Zanazzi–Jona,  $R_{\text{P}}$ : Pendry  $R$  factor) of integral and extra beams in the  $(2 \times 1)$  structure as function of the spacing between first and second Fe layer.

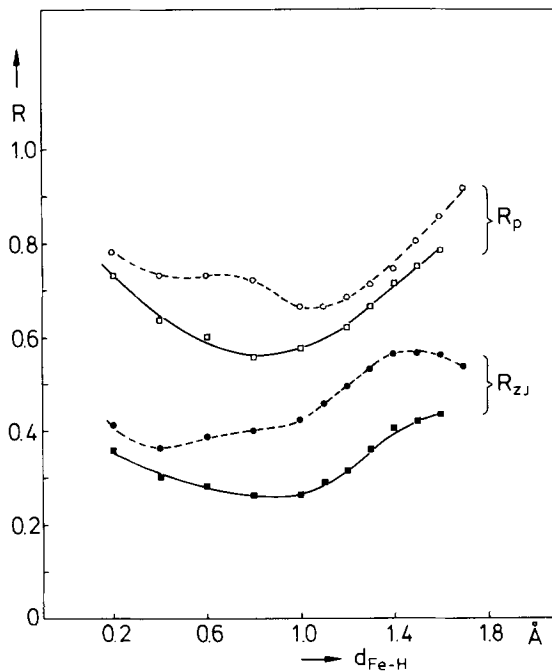


FIG. 7. Averaged  $R$  factor of extra beams alone in the  $(2 \times 1)$  structure as function of the layer spacing between Fe and H for long bridge site (---) and threefold site (—).

scattering effects and these are weak for hydrogen.

The top iron layer spacing, a variation of which has a strong effect on all beams, is found to be close to the bulk value. A deviation from the bulk value or a difference to the result of the clean surface is certainly below the error limits of this study.

### B. $(3 \times 1)$ structure

Experimental  $I$ - $V$  data were taken at normal incidence and at  $\theta = 11.3^\circ$  and  $\varphi = 90^\circ$ , altogether 11 spectra—seven superstructure beams and four integer order beams. Calculations were performed for three models which remained possible after the analysis of the  $(2 \times 1)$  structure. These were the long bridge site model and two threefold hollow site models. In addition also the top site model was analyzed in order to get an estimate how sensitive the spectra react with respect to the adsorption site. Again, as for the  $(2 \times 1)$  structure the top site could be ruled out by visual comparison.

If the H atoms are adsorbed on the long bridge sites there is only one possibility to construct a  $(3 \times 1)$  structure for a coverage of  $\theta = 2/3$ . It is derived from a  $(1 \times 1)$  structure where every third chain of hydrogen atoms is removed. The symmetry of the structure model is  $2mm$  and, besides antiphase domains, only one domain can exist [see Fig. 3(c)]. For the threefold hollow site two possible structures are conceivable. One has been proposed by Muscat,<sup>3</sup> [see Fig. 3(e)], it has the symmetry  $2m$  and consequently two domains are required to be consistent with the  $2mm$  symmetry of the diffraction pattern. This model (II) is obtained from the long bridge site model by shifting the whole hydrogen layer to one side of the bridge position.

Another model (I), which seems more appropriate, can be constructed by placing the hydrogen atoms alternately

into the threefold sites. The symmetry of this structure is  $2mm$  and only one domain is necessary [see Fig. 3(d)].

A comparison of some of the experimental data with the three theoretical curves is shown in Fig. 8. As can be seen none of the models gives a convincing agreement with the experimental curves. Several calculated beams fit the experiment quite well, others give only poor agreement. This conclusion is also underlined by the  $R$  factor analysis (see Fig. 9). The best model is the threefold site with alternate occupation of the two hollow sites [Fig. 3(d)]. Here the minimum  $R$  factors of only superlattice beams are  $R_{ZJ} = 0.40$  and  $R_P = 0.58$ . The corresponding values for the other threefold site model are  $R_{ZJ} = 0.45$  and  $R_P = 0.58$ . The long bridge site leads to much worse values  $R_{ZJ} = 0.6$  and  $R_P = 0.74$ .

Again, as for the  $(2 \times 1)$  structure, the long bridge site seems more unlikely than the threefold sites, though the agreement for the other two models is also not very satisfactory. A clear distinction between the two threefold site models cannot be made on the basis of the LEED data alone.

In contrast to the  $(2 \times 1)$  structure here a clear difference between the calculations for the threefold site and the long bridge site occurs. This may be explained by the fact that the density of hydrogen atoms is higher for the  $(3 \times 1)$  structure. Although the geometry within the hydrogen layer is different for both structure models with the threefold site, the  $I/V$  curves are rather similar and more pronounced differences occur with respect to the long bridge site model. A prefer-

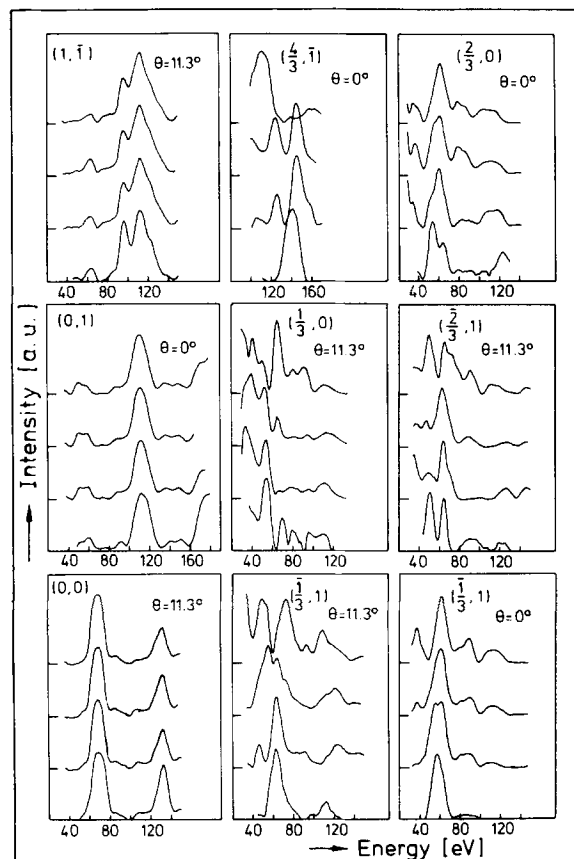


FIG. 8.  $I/V$  curves of the  $(3 \times 1)$  structure, beams and polar angle of incidence as indicated ( $\varphi = 90^\circ$ ). Order of curves in each set from bottom to top: experimental; threefold site, model I; threefold site, model II; long bridge site.

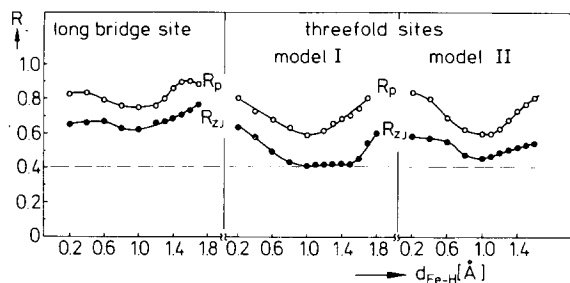


FIG. 9. Averaged  $R$  factors of the extra beams alone in the  $(3 \times 1)$  structure as function of the layer spacing between Fe and H for long bridge site, threefold site in model I and threefold site in model II.

ence for one adsorption site therefore can be found. Indeed the  $R$  factors for the long bridge site model are significantly higher. As the same result has been found for the  $(2 \times 1)$  structure—though the decision was not so clear in that case—we conclude that the long bridge site model can be ruled out.

Despite the rather poor  $R$  factor, these results are expected to be reliable due to the following reasons: The structural parameters—the Fe–Fe and the Fe–H interlayer spacing—come out identical to those obtained for the  $(2 \times 1)$  structure  $d_{\text{Fe-Fe}} = 2.0 \text{ \AA}$  and  $d_{\text{Fe-H}} = 0.9\text{--}1.1 \text{ \AA}$ . In addition both  $R$  factors exhibit minima at these point.

### C. Influence of disorder on $I/V$ profiles

It seems very likely that the H atoms are at least partially delocalized between the two adjacent threefold sites. The distance between them is very small ( $1.01 \text{ \AA}$ ) and the energy barrier which is simply the difference in adsorption energy for the threefold site and the long bridge site should lie within the thermal energy range. Theoretical evidence for this latter conclusion will be discussed in some more detail later.

Such delocalization effects could explain the high mobility of the chemisorbed hydrogen atoms that has been observed experimentally and would give rise to strong fluctuations in the short-range order of the H overlayer. These fluctuations have some implications on the  $I/V$  curves and on the average intensities. In the case of a completely statistical occupation of both threefold sites aside the long bridge sites, the LEED beams should remain sharp, embedded in a diffuse background. The sharp reflections are due to the fact that only lattice sites can be occupied. In the case considered here only one-dimensional disorder would occur—in  $[1\bar{1}0]$  direction (see Fig. 3)—which would in principle be observable by a streak in the diffraction pattern along that direction. The streaks would hardly be detectable since hydrogen is a weak scatterer and the streak certainly would be hidden in the background produced by other defects.

Therefore, from the observation of the diffraction pattern and also from the result of the LEED intensity analysis it cannot be excluded that the structure is highly disordered and we have to investigate that possibility here too. We need to consider here only the two limiting cases, that means either perfect order or complete random occupation of the respective neighbored threefold sites. The perfect order, with large domains of low-symmetry superstructures, re-

quires averaging of intensities what has already been done in the above analysis. Thus we only need to investigate whether complete random occupation of the neighbored threefold sites would give a better agreement between the experimental and theoretical curves. The random occupation requires the coherent summation of scattering amplitudes. The kinematic theory would give here only a scaling factor to the  $I/V$  profiles, but differences occur due to multiple-scattering effects. The implications of domain distributions on the precision of a structure analysis by LEED have been recently discussed by Jagodzinski.<sup>30</sup>

The intensity scattered from a surface with random occupation of one or more different adsorption sites can be divided into two parts, describing a sharp reflection and a diffuse background.

$$I(\mathbf{k}, \mathbf{k}') = I_s(\mathbf{k}, \mathbf{k}') + I_d(\mathbf{k}, \mathbf{k}')$$

We may consider here only the sharp reflection

$$I_s(\mathbf{k}, \mathbf{k}') = R \cdot \frac{\sin^2(N_1 \cdot \pi \cdot h)}{\sin^2(\pi \cdot h)} \cdot \frac{\sin^2(N_2 \cdot \pi \cdot k)}{\sin^2(\pi \cdot k)} |\bar{F}|^2.$$

The sharp reflection results from the fact that the pair correlation function for two adsorbate atoms does not vanish at large distances, but approaches an average value.  $R$  is a normalization constant,  $h$  and  $k$  are the indices of the beam, and  $N_1$  and  $N_2$  are the number of scatterers in each direction.

$$|\bar{F}|^2 = \left| \sum_{\nu} p_{\nu} F_{\nu}(\mathbf{k}, \mathbf{k}') \right|^2$$

is the average amplitude,  $\mathbf{k}$  and  $\mathbf{k}'$  are the wave vectors of the incident and scattered beam, respectively. The scattering amplitudes  $F_{\nu}(\mathbf{k}, \mathbf{k}')$  of the different unit cells here represent the sum over all layers and also include all multiple-scattering events in the bulk. For the sake of simplicity, we neglect here multiple-scattering events within the hydrogen layer. The  $p_{\nu}$  denote the *a priori* occupation probabilities in the unit cell  $\nu$ . We will investigate here only the  $(2 \times 1)$  structure, since in that case no phase factor between the different scattering amplitudes occurs: The domain vector, which separates two domains, is zero. In the  $(3 \times 1)$  structure this is not true. We then assume  $p_{\nu} = 0.5$  for the two possible threefold sites. Finally we only need to add up the scattering amplitudes for both domains, which were already calculated in the computer program.

At normal incidence the intensity of the  $(\frac{1}{2}, 1)$  beam remains unaltered since the lattice spacing in  $[001]$  direction is well ordered. In other words, the  $(\frac{1}{2}, 1)$  beam does not “see” the disorder. Only the  $I/V$  curve for the  $(\frac{1}{2}, 0)$  beam should be affected. However, it should be noted that the influence on  $I/V$  curves is purely due to multiple-scattering effects. In the kinematic limit all structure models for the  $(2 \times 1)$  structure and also for a disordered structure would produce the same  $I/V$  curves for superstructure beams, apart from a scaling factor. Consequently major differences between averaged amplitudes and averaged intensities were only found in cases where the long bridge site and the threefold site produced different  $I/V$  curves. In all cases it was found that the agreement between theoretical and experimental spectra was significantly worse for a disordered structure and averaged amplitudes than for two large ordered domains and averaged

intensities. This result means that from the LEED intensity analysis no evidence is found for a random occupation of both neighboring sites. On the contrary, the theoretical results seem to fit the experimental data better if only a single adsorption site is assumed. But the agreement between theory and experiment is too poor to completely exclude any disorder.

Random occupation of both threefold sites would not only change the  $I/V$  curves of certain fractional order beams, but would also introduce a scaling factor in the average intensity. The threefold site approximately has the coordinates  $(3/4, 3/8)$  in the unit cell and the averaged scattering amplitude of a superstructure beam in the kinematic approximation would be given by

$$|F(\mathbf{k}, \mathbf{k}')| = \frac{1}{2} | \{ f_{\text{H}}(\mathbf{k}, \mathbf{k}') e^{2\pi i(\frac{3}{4}h + \frac{3}{8}k)} + f_{\text{H}}(\mathbf{k}, \mathbf{k}') e^{2\pi i(-\frac{3}{4}h - \frac{3}{8}k)} \} |$$

$$= \frac{1}{2} f_{\text{H}}(\mathbf{k}, \mathbf{k}') \quad \text{for } h = \frac{1}{2}, \quad k = 0,$$

$$= f_{\text{H}}(\mathbf{k}, \mathbf{k}') \quad \text{for } h = -\frac{1}{2}, \quad k = 1$$

since the Fe atoms do not contribute to the intensity in the extra beams. Strictly, this argument is only valid in the kinematic theory, but should be qualitatively applicable in the multiple-scattering calculation as well. On the average, over a sufficient large energy range, no extra intensity is produced by multiple scattering.

The above result means that the scaling factor of the  $(\frac{1}{2}, 0)$  beam should be approximately one-quarter of that of the  $(\frac{1}{2}, 1)$  beam. Such an effect was not observed. The scaling factor between measured and calculated intensities varies for all beams from 0.5–0.3, also for the integer order beams, which indicates relatively little disorder within the hydrogen layer.

For the two cases investigated, complete statistical occupation of both sites and well ordered large domains, sharp diffraction spots are expected. In contrast, short-range disorder including a correlation for the occupation of two neighboring sites would produce broadened beams. Experimentally such broadening is not observed, the average domain size thus must be at least 10–15 superlattice spacings. From the low scattering power of hydrogen and the relatively small differences between the curves of averaged amplitudes and averaged intensities it can be concluded that such disorder would not affect the  $I/V$  curves substantially. It is therefore very unlikely that some degree of disorder within the hydrogen layer is responsible for the remaining discrepancies between theoretical and experimental curves.

## V. DISCUSSION

Despite the widespread interest in the properties of adsorbed hydrogen, to our knowledge so far only one report on a successful LEED structural analysis [for H/Ni (111)] can be found in the literature.<sup>12</sup> Apart from this, a structure analysis for H/Ni (110) was performed by He diffraction<sup>13</sup> whose essential features are confirmed by a current LEED study in our laboratory.<sup>14</sup> This lack is certainly caused by the fact that H is a weak scatterer which makes the intensities small and may lead to computational problems. In fact there was a long controversy whether extra beams could be caused by an ordered hydrogen structure itself or whether it necessarily demands a hydrogen induced reconstruction of the metal. In

that case the extra beams are caused by the structure of the metal atoms. The structure determination for H on Ni (111) proved that adsorbed H itself can cause the appearance of clearly visible extra beams of an ordered superstructure.<sup>12</sup>

As an example for the second case earlier attempts to analyze the LEED data from the room-temperature H/Ni (110) phase indicated strongly the occurrence of surface reconstruction, although a determination of this structure was not possible.<sup>31</sup> This failure illustrates the general problem (or better inability) to determine the position of a weak scatterer-like hydrogen if the superstructure is also due to a respective arrangement of heavy (i.e., substrate) atoms. Examples of this kind are the hydrogen induced reconstructions of the metal surface, e.g., observed for Pd (110),<sup>32</sup> Ni (110),<sup>13,31,33</sup> W (100),<sup>34</sup> and W (110),<sup>35</sup> but also the ordered layers of adsorbed hydrocarbons. A LEED based structure analysis of the latter omits the hydrogen atoms completely.<sup>36</sup> The analysis of the present system did not show any evidence for a hydrogen induced reconstruction or relaxation of the Fe–Fe layer spacing. Rather it could clearly be demonstrated from the behavior of the integral  $I/V$  curves upon adsorption as well as from the total intensity of the extra beams that they are caused by the ordered hydrogen adlayer itself, as for H/Ni (111). Both substrate surfaces Fe (110) and Ni (111) are in their crystal structures (bcc and fcc, respectively) closest packed metal planes which are known to be relatively stable against an adsorbate induced reconstruction. Consequently, for the two other examples of an ordered H adlayer on such a plane, the  $(\sqrt{3} \times \sqrt{3})R 30^\circ$  structures on Pd (111)<sup>37</sup> and the  $(1 \times 1)$  structure on Pt (111),<sup>16</sup> a reconstruction is also excluded.<sup>38,16</sup> In the present case also no adsorbate induced variation of the spacing between the topmost substrate layers was found. This is presumably due to the fact that in the clean Fe (110) surface this spacing is very close to the bulk value. [Effects of this type occur, on the other hand, in hydrogen adsorption on the more open Ni (110) plane.<sup>14</sup>]

The LEED analysis of the graphitic  $(2 \times 2)$  H structure on Ni (111)<sup>12</sup> was carried out without determination of  $R$  factors which the authors thought would be misleading as the integral order beams contain little or no structural information from the hydrogen overlayer and only three superstructure beams were available. Based on visual comparison the degree of agreement between experimental and computed  $I/V$  curves is about the same level as in our study. The structure of the spectra is in most cases reproduced quite well, but toward higher energies the differences become greater.

In the present work an exclusion of some structural models could already be made from visual inspection of the spectra, but for a distinction between the threefold site and the long bridge site the  $R$  factor analysis proved to be quite useful. Both adsorption sites give quite similar spectra and only the  $R$  factor analysis reveals that the threefold coordinated site has to be considered as the actual location of the hydrogen atom.

The Zanazzi–Jona  $R$  factor from all beams—integral and half-order spots—comes close to a value of 0.2 for the  $(2 \times 1)$  phase. The superstructure beams alone for this phase result in an  $R$  factor of  $R_{21} \approx 0.25$ , so that the structural

result from this phase can be judged with some confidence. Considering only the superstructure beams for the  $(3 \times 1)$  phase, the best agreement between theoretical and experimental  $I/V$  spectra comes out much worse with an average  $R_{Zj}$  factor of about 0.4 for model I. The minimum, however, is reached for the same structural parameters as for the  $(2 \times 1)$  phase, which gives some more confidence in structural result for the  $(3 \times 1)$  structure.

The unsatisfactory high  $R$  factor in this [and in the H/Ni (111)] study does certainly not result from the use of too few phase shifts at higher energies. More plausible are two other reasons: The scattering potential in the muffin tin approach as well as the vibrational amplitudes are isotropic, which clearly is a simplification of the real situation. These effects become more important at higher energies since here the contribution of the higher  $l$  values of the phase shifts are larger.<sup>39</sup> Therefore we believe that the higher  $R$  factor for the  $(3 \times 1)$  structure does not result from a false structural model but primarily from an inappropriate hydrogen potential and further nonstructural parameters. These deviations more heavily affect the  $(3 \times 1)$  than the  $(2 \times 1)$  structure because of its higher coverage and larger unit cell.

In addition to the analysis of LEED intensities there are several other experimental techniques which provide information about the adsorption geometry and which were used to investigate hydrogen adlayers, e.g., He diffraction [H/Pd (110),<sup>40</sup> H/Ni (110),<sup>13</sup> H/Pt (111)<sup>16</sup>], ARUPS [H/Ni (111),<sup>41</sup> H/Pd (111),<sup>41</sup> H/Pt (111)<sup>41</sup>], or vibrational spectroscopies [H/Ni (110),<sup>15</sup> H/Pt (111),<sup>17</sup> H/Fe (110),<sup>5</sup> H/Pd (100),<sup>42</sup> H/Ni (100),<sup>43</sup> H/Ni (111)<sup>44</sup>.] Of direct relevance to the present study are the vibrational data determined for H/Fe (110) by HREELS. Baró and Erley<sup>5</sup> observed two frequencies: one under specular conditions at  $1060 \text{ cm}^{-1}$  and a second band at  $880 \text{ cm}^{-1}$  under nonspecular conditions. The vibrational frequency of an H atom bound linearly to a metal atom would appear at a much higher value than observed, so that the on top site was excluded. From the dipole selection rule the authors concluded that the vibrational band at  $1060 \text{ cm}^{-1}$  belongs to the excitation of the symmetric stretching mode of bridge bonded hydrogen, whereas the lower frequency was attributed to the asymmetric stretching mode. Using a simple relationship between the M–H–M bond angle and their ratio of the symmetric to the asymmetric stretching mode frequency and assuming a M–H bond length in the range of 1.5–2.0 Å the authors concluded that the short bridge is the adsorption site for the H atom, which definitely can be ruled out from our LEED analysis. We believe that the HREELS results were misinterpreted for the following reasons: First of all the authors were mistaken in assigning a symmetry  $C_1$  to H adsorbed on the threefold site, which correctly is  $C_s$ . Secondly, Nordlander *et al.* have recently pointed out that on smooth metal surfaces hydrogen cannot be treated in a harmonic approach.<sup>45</sup> Puska *et al.* have performed detailed calculations of excitation frequencies for hydrogen on Ni, in which the hydrogen is described in a delocalized picture forming energy bands.<sup>46</sup> As a consequence, analysis of vibrational spectra in terms of localized force models may be rather misleading.

In two theoretical studies the adsorption energy and

bonding of hydrogen on Fe (110) was investigated. Pasco and Ficalora<sup>47</sup> performed a Bond Energy–Bond Order model calculation and suggested that the  $(2 \times 1)$  structure is formed by an adsorbed  $\text{H}_2^+$  ion. This interpretation, which is unphysical already from the  $\text{H}_2$  ionization level far below  $E_F$  ( $I_p \approx 15.3 \text{ eV}$ <sup>48</sup>), is most easily dismissed from the HREELS results, which clearly rule out any molecular adsorbate. The other study by Muscat<sup>11</sup> used an embedded cluster formalism and resulted in an identical adsorption geometry as ours. The H atoms are preferentially adsorbed in the threefold coordinated sites. On the basis of the interaction energies between chemisorbed H his atoms model predicts formation of a graphitic  $(2 \times 2)$  structure for smaller H–Fe bond lengths (1.59 Å) and of a  $(2 \times 1)$  structure for larger H–Fe distances (1.78 Å). In view of our results, which give a Fe–H bond length of  $1.75 + 0.05 \text{ Å}$ , the theoretical predictions agree quite well with the experimental findings.

Two other calculations should be mentioned which bear close resemblance to our system. Blyholder *et al.* simulated H adsorption on Fe (100) and performed MINDO calculations on a  $\text{Fe}_{12}\text{H}$  cluster.<sup>49</sup> According to these calculations the most stable site is again the threefold coordinated site, not a bridge bonded or a fourfold coordinated site. Nordlander *et al.*<sup>45</sup> found like Muscat<sup>11</sup> a general trend for hydrogen to adsorb in the highly coordinated sites. For W (110), which has the same symmetry as Fe (110), the threefold sites were identified as being the most stable ones. In this work it was further concluded that the adsorbed H atoms have a very low diffusion barrier, since bridge sites are not so much higher in energy. In particular the energy difference between long bridge and threefold sites is so small that pronounced delocalization of the adsorbed H atoms is predicted. These latter effects were recently investigated in more detail for H on the low index planes of nickel. Energetically quite similar effects as for H/W (110) are also expected for H/Fe (110).<sup>50</sup>

The concept of “band-like” states for the adsorbed H atoms would for example account for their high surface mobility, but most probably only holds for diluted systems: The observation of different ordered H overlayer structures by LEED demonstrates that the interaction energies between the adsorbed particles causes their fixation to specific adsorption sites. This is also supported by the  $I/V$  analysis as discussed above.

As a consequence of the higher electronegativity of the H atom in comparison with the Fe atom a slightly negatively charged  $\text{H}_{\text{ad}}$  would be expected. Experimentally a decrease of the work function at hydrogen adsorption up to a value of  $-85 \text{ mV}$  at saturation coverage is found.<sup>2</sup> In terms of a point dipole picture this would contradict the above conclusions, but one has to bear in mind that the work function changes results not only from a charge transfer between metal and adsorbate atoms but also from a rearrangement of the charge distribution within the metal surface and in the bond region between H atoms and metal. A slight decrease of the work function therefore is conceivable. Also the Fe–H distance points to a negatively charged adsorbed particle: From the  $R$  factor analysis a minimum is obtained for a Fe–H bond length between 1.70 and 1.80 Å, which is longer than the sum of the covalent radii of 1.59 Å.



For H/Ni (111)<sup>12</sup> a H metal bond length of 1.84 Å has been determined which is close to the value of  $1.75 \pm 0.05$  Å obtained for the present system. The structure of an iron-hydrogen cluster compound has been determined by a neutron diffraction study.<sup>51</sup> In this case the H atom is bridge bonded with a H-Fe bond length of 1.67 Å to two Fe atoms that are separated by 2.60 Å. This Fe-H distance thus is not very far from the structural parameters of the adsorbate complex on Fe (110).

The ordered H structures on Ni (111)<sup>12</sup> and Pd (111)<sup>36</sup> exhibit rather constant H-H distances, which is due to the isotropic substrate geometry and the rapidly increasing repulsion between H atoms at closer distances. Of the two kinds of threefold sites on these surfaces both are occupied on the graphitic (2×2) on Ni (111), while only one is used in the two ( $\sqrt{3} \times \sqrt{3}$ )R 30° structures on Pd (111). On Fe (110) only one type of threefold sites exists and it was pointed out by Muscat that at shorter Fe-H distances a graphitic like (2×2) configuration would be most stable.<sup>11</sup> The anisotropic situation on the Fe (110) surface becomes evident from the calculated H-H pairwise interaction energies<sup>11</sup> shown in Fig. 10. Especially  $E_1$  is only slightly repulsive and makes the formation of the dense H rows in [001] direction possible. These arguments shall be used as further support for model I for the (3×1) structure. Using Muscat's nomenclature and values for the interaction energies these would total for model II to

$$E_{\text{H-H}} = 2E_1 + 2E_3 + E_4,$$

$$E_{\text{H-H}} = 37 \text{ meV}$$

per unit cell. For model I two additional interaction energies, which were not included in the calculations, are indicated as  $E_5$  and  $E_6$  in Fig. 10. The total interaction energy per unit cell in model I then amounts to

$$E_{\text{H-H}} = 2E_1 + 2E_5 + E_6.$$

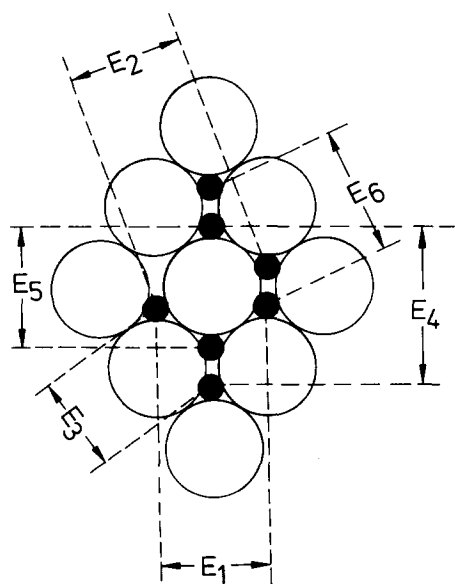


FIG. 10. Pairwise H-H interaction energies on Fe (110):  $E_1$ - $E_4$  from Ref. 11,  $E_5$  and  $E_6$  introduced here ( $E_1 = +3.5$  meV,  $E_2 = +10.4$  meV,  $E_3 = +14.0$  meV, and  $E_4 = +2.0$  meV for  $d_{\text{Fe-H}} = 1.78$  Å).

This structure also exploits the energetically "cheap" arrangement in close-packed rows along the [001] direction. The interaction energy  $E_6$  is estimated to be slightly stronger repulsive than  $E_4$ . The energetic gain really stems from avoiding the highly repulsive interaction energies  $E_3$  within the double rows and this presumably is much more than the loss by going from  $E_4$  to  $E_6$ . In this picture model I consequently is more stable if

$$2E_5 + E_6 < 2E_3 + E_4.$$

In a more precise description certainly also trio interactions have to be included. But also then the main point in this argument is not expected to change. The energy gain by avoiding the highly repulsive interaction  $E_3$  between neighboring rows, which also stabilizes the (2×1) structure, should not be overcompensated by trio interactions. These arguments rather than the small differences in the  $R$  factor led us to favor the model I for the (3×1) structure.

The 2D phase diagram mapped out by Kinzel *et al.*<sup>7-10</sup> is based on the assumption of a long bridge adsorption site, which was used by the authors of Refs. 3 and 6 as well. There exist, in fact, twice as many threefold sites than long bridge sites, which will certainly require more and presumably different interaction energies. We expect, however, that these will be of the same order of magnitude, as indicated by comparison with other systems using the higher number of threefold sites.<sup>37,38</sup> The conclusions with respect to the trio interactions have to be altered, however, A 2D system with only pairwise interactions should exhibit a phase diagram symmetric to one-half of the possible sites. For the long bridge site this would require symmetry with respect to  $\theta = 0.5$ . Since the experimental phase diagram does not exhibit this symmetry this was used as a direct proof for the existence of nonpairwise, e.g., trio interactions. For the threefold site symmetry would only be required with respect to  $\theta = 1.0$  and so H/Fe (110) can no longer be regarded as a direct example for trio interactions, if this conclusion is merely based on the symmetry of the 2D phase diagram.

## VI. CONCLUSIONS

In this LEED intensity analysis of H/Fe (110) we have clearly identified the threefold sites as adsorption site for the adsorbed hydrogen atom. The H-Fe bond length was determined to  $1.75 \pm 0.05$  Å, equivalent to an interlayer spacing of  $0.9 \pm 0.1$  Å. A hydrogen induced reconstruction and, within the accuracy of this study, also a relaxation of the substrate could be excluded, the extra beams are solely due to an ordered H adlayer. As becomes evident from the beam profiles and their relative intensities the structure exhibits rather good long-range order. No indication for short-range fluctuation due to a delocalization of the H over the two neighbored threefold sites was observed, despite of the high mobility of single atoms. The H atoms consequently are localized at lattice sites due to the interactions between adsorbed particles. The (3×1) structure at  $\theta = 2/3$  contains two H atoms per unit cell for the two models which were discussed. We favor the more regular configuration of model I rather than the formation of double rows as in model II. This conclusion cannot be drawn from the small difference

between the respective  $R$  factors alone, but is based also on qualitative arguments about the interaction energies and on comparison with the structures of other ordered H adlayers.

## ACKNOWLEDGMENTS

We gratefully acknowledge support from the Deutsche Forschungsgemeinschaft (SFB 128) and from the Bavarian Academy of Science, which provided the computing facilities. One of us (T. M.) is grateful for a Humboldt fellowship.

- <sup>1</sup>K. Christmann, Surf. Sci. Rep. (in preparation).  
<sup>2</sup>J. Benzinger and R. J. Madix, Surf. Sci. **94**, 119 (1980).  
<sup>3</sup>F. Boszo, G. Ertl, M. Grunze, and M. Weiss, Appl. Surf. Sci. **1**, 103 (1977), and references there to earlier work.  
<sup>4</sup>R. Dziembaj and G. Wedler, Surf. Sci. **134**, 283 (1983).  
<sup>5</sup>A. M. Baró and W. Erley, Surf. Sci. **112**, 1759 (1981).  
<sup>6</sup>R. Imbihl, R. J. Behm, K. Christmann, G. Ertl, and T. Matsushima, Surf. Sci. **117**, 257 (1982).  
<sup>7</sup>W. Kinzel, W. Selke, and K. Binder, Surf. Sci. **121**, 13 (1982).  
<sup>8</sup>W. Selke, K. Binder, and W. Kinzel, Surf. Sci. **125**, 74 (1983).  
<sup>9</sup>W. Kinzel, Phys. Rev. Lett. **51**, 996 (1983).  
<sup>10</sup>K. Binder, W. Kinzel, and D. P. Landau, Surf. Sci. **117**, 232 (1982).  
<sup>11</sup>J. -P. Muscat, Surf. Sci. **118**, 321 (1982); **110**, 389 (1981).  
<sup>12</sup>K. Christmann, R. J. Behm, G. Ertl, M. A. Van Hove, and W. H. Weinberg, J. Chem. Phys. **70**, 4168 (1979).  
<sup>13</sup>K. H. Rieder and T. Engel, Phys. Rev. Lett. **43**, 373 (1979); **45**, 824 (1980).  
<sup>14</sup>W. Reimer, W. Moritz, R. J. Behm, G. Ertl, and V. Penka (to be published).  
<sup>15</sup>N. J. DiNardo and E. W. Plummer, J. Vac. Sci. Technol. **20**, 890 (1982); L. Ollé and A. M. Baró, Surf. Sci. **137**, 607 L (1984); M. Nishijima, S. Masuda, H. Kobayashi, and M. Onchi, Rev. Sci. Instrum. **53**, 790 L (1982); M. Nishijima, S. Masuda, M. Jo, and M. Onchi, J. Electron. Spectrosc. Related Phenomena **29**, 273 (1983).  
<sup>16</sup>J. Lee, J. P. Cowin, and L. Wharton, Surf. Sci. **130**, 1 (1983).  
<sup>17</sup>A. M. Baró, H. Ibach, and H. D. Bruchmann, Surf. Sci. **88**, 384 (1979).  
<sup>18</sup>E. Lang, P. Heilmann, G. Hanke, K. Heinz, and K. Müller, Appl. Phys. **19**, 287 (1979).  
<sup>19</sup>H. D. Shih, F. Jona, U. Bardi, and P. M. Marcus, J. Phys. C **13** 3801 (1980).  
<sup>20</sup>M. A. Van Hove and S. Y. Tong, *Surface Crystallography by LEED*, Springer Series in Chemical Physics (Springer, Berlin, 1979).  
<sup>21</sup>W. Moritz, J. Phys. C **17**, 353 (1984).  
<sup>22</sup>V. L. Moruzzi (personal communication).  
<sup>23</sup>K. O. Legg, F. Jona, D. W. Jepsen, and P. M. Marcus, J. Phys. C **10**, 937 (1977).  
<sup>24</sup>H. D. Shih, F. Jona, D. W. Jepsen, and P. M. Marcus, Surf. Sci. **104**, 33 (1981).  
<sup>25</sup>R. Imbihl, R. J. Behm, G. Ertl, and W. Moritz, Surf. Sci. **123**, 129 (1982).  
<sup>26</sup>*International Tables of X ray Crystallography* (Kynoch, Birmingham, 1962), Vol. III.  
<sup>27</sup>E. Zanazzi and F. Jona, Surf. Sci. **60**, 445 (1976).  
<sup>28</sup>J. P. Pendry, J. Phys. C **13**, 937 (1980).  
<sup>29</sup>V. V. Gonshar, O. V. Kanash, A. G. Nauvometts, and A. G. Fedorus, JETP Lett. **28**, 61 (1978).  
<sup>30</sup>H. Jagodzinski, Z. Naturforsch. Teil A **37**, 1103 (1982).  
<sup>31</sup>J. E. Demuth, J. Colloid Interface Sci. **58** 184 (1977).  
<sup>32</sup>M. G. Cattania, V. Penka, K. Christmann, R. J. Behm, and G. Ertl, Surf. Sci. **128**, 367 (1982).  
<sup>33</sup>V. Penka, K. Christmann, and G. Ertl, Surf. Sci. **136**, 307 (1984).  
<sup>34</sup>R. A. Barker and P. J. Estrup, J. Chem. Phys. **74**, 1442 (1981); D. A. King and G. Thomas, Surf. Sci. **92**, 201 (1980), and references therein.  
<sup>35</sup>J. W. Chung and P. J. Estrup, 44th Annual Conference on Physical Electronics, Princeton, 1984.  
<sup>36</sup>R. F. Lin, R. J. Koestner, M. A. Van Hove, and G. A. Somorjai, Surf. Sci. **134**, 161 (1983).  
<sup>37</sup>T. E. Felter, S. M. Foiles, M. S. Daw, and R. H. Stulen, in *The Structure of Surfaces*, edited by M. A. van Hove and S. Y. Tong, Springer Series in Surface Science (Springer, Berlin, 1985).  
<sup>38</sup>R. Stulen (personal communication).  
<sup>39</sup>J. B. Pendry, *Low Energy Electron Diffraction* (Academic, New York, 1974).  
<sup>40</sup>K. H. Rieder, M. Baumberger, and W. Stocker, Phys. Rev. Lett. **51**, 1799 (1983).  
<sup>41</sup>W. Eberhard, F. Greuter, and E. W. Plummer, Phys. Rev. Lett. **46**, 1085 (1981).  
<sup>42</sup>C. Nyberg and C. G. Tengstal, Surf. Sci. **126** 163 (1983).  
<sup>43</sup>S. Anderson, Chem. Phys. Lett. **55**, 185 (1978).  
<sup>44</sup>H. Ibach and D. Bruchmann, Phys. Rev. Lett. **44**, 36 (1980); W. Ho, N. J. DiNardo, and E. W. Plummer, J. Vac. Sci. Technol. **17**, 134 (1980).  
<sup>45</sup>P. Nordlander, S. Holloway, and J. K. Nørskov, Surf. Sci. **136**, 59 (1984).  
<sup>46</sup>M. J. Puska, R. M. Nieminen, M. Manninen, B. Chakraborty, S. Holloway, and J. K. Nørskov, Phys. Rev. Lett. **51**, 1081 (1983).  
<sup>47</sup>R. W. Pasco and P. J. Ficalora, Surf. Sci. **134**, 476 (1983).  
<sup>48</sup>*CRC Handbook of Physics and Chemistry* (CRC, Cleveland, 1967).  
<sup>49</sup>G. Blyholder, J. Head, and F. Ruetter, Surf. Sci. **131**, 403 (1983).  
<sup>50</sup>J. K. Nørskov (personal communication).  
<sup>51</sup>M. W. Howard, U. A. Jayasooriya, S. F. A. Kettle, D. B. Powell, and N. Sheppard, Chem. Commun. **929**, 18 (1979); U. A. Jayasooriya, M. A. Chesters, M. W. Howard, S. F. A. Kettle, D. B. Powell, and N. Sheppard, Surf. Sci. **93**, 526 (1980).

The Journal of Chemical Physics is copyrighted by the American Institute of Physics (AIP). Redistribution of journal material is subject to the AIP online journal license and/or AIP copyright. For more information, see <http://ojps.aip.org/jcpo/jcpcr/jsp>  
Copyright of Journal of Chemical Physics is the property of American Institute of Physics and its content may not be copied or emailed to multiple sites or posted to a listserv without the copyright holder's express written permission. However, users may print, download, or email articles for individual use.